Anisotropic Structure of Calcium-Induced Alginate Gels by Optical and Small-Angle X-ray Scattering Measurements

ARTICLE *in* BIOMACROMOLECULES · JUNE 2011

Impact Factor: 5.75 · DOI: 10.1021/bm200223p · Source: PubMed

9 AUTHORS, INCLUDING:

Kazuya Furusawa
Hokkaido University
29 PUBLICATIONS **181** CITATIONS

SEE PROFILE

Katsuzo Wakabayashi
Osaka University
160 PUBLICATIONS **1,881** CITATIONS

SEE PROFILE

Biomacromolecules

ARTICLE

pubs.acs.org/Biomac

Anisotropic Structure of Calcium-Induced Alginate Gels by Optical and Small-Angle X-ray Scattering Measurements

Yasuyuki Maki,*[,†] Kei Ito,[†] Natsuki Hosoya,[†] Chikayoshi Yoneyama,[†] Kazuya Furusawa,[†] Takao Yamamoto,[†] Toshiaki Dobashi,[†] Yasunobu Sugimoto,[‡] and Katsuzo Wakabayashi[‡]

[†]Department of Chemistry and Chemical Biology, Graduate School of Engineering, Gunma University, Kiryu 376-8515, Japan

[‡]Division of Biophysical Engineering, Graduate School of Engineering Science, Osaka University, Toyonaka, Osaka 560-8531, Japan

ABSTRACT: It was more than 50 years ago that an appearance of birefringence in alginate gels prepared under cation flow was reported for the first time, however, the anisotropic structure of the alginate gel has not been studied in detail. In the present study, anisotropic Ca-alginate gels were prepared within dialysis tubing in a high Ca^{2+}-concentration external bath, and optical and small-angle X-ray scattering (SAXS) measurements were performed to characterize the structure of the gel. The observations of the gel with crossed polarizers and with circular polarizers revealed the molecular orientation perpendicular to the direction of Ca^{2+} flow. Analyses of the SAXS intensity profiles indicated the formation of rod-like fibrils consisting of a few tens of alginate molecules and that the anisotropy of the gel was caused by the circumferential orientation of the large fibrils. From the observed asymmetric SAXS pattern, it was found that the axis of rotational symmetry of the anisotropic structure was parallel to the direction of Ca^{2+} flow. The alignment factor (A_f) calculated from the SAXS intensity data confirmed that the orientation of the fibrils was perpendicular to the direction of Ca^{2+} flow.

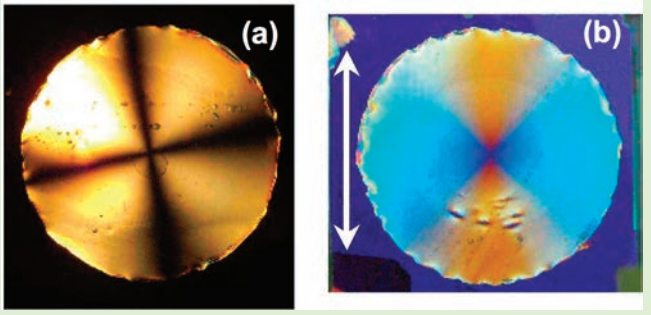

1. INTRODUCTION

Alginates are polysaccharides mainly isolated from brown algae. They are linear copolymers consisting of two kinds of uronic acids, β-D-mannuronic acid (M) and α-L-guluronic acid (G), forming regions of M-, G-, and MG-blocks of alternating structure. Alginates are widely used in industries such as food, pharmaceutical, and biomedical as solution property modifiers and gelling agents.[1,2]

Due to its industrial applications, numerous studies have been devoted to clarify the gelling properties of alginate. Aqueous solutions of alginate form hydrogels in the presence of various divalent cations such as Ca^{2+}, Cu^{2+}, and Ba^{2+}. For the preparation of the cation-induced alginate gels, there are two fundamental methods to introduce cross-linking in a controlled manner:[1,2] the diffusion setting method and the internal setting method. The diffusion setting method is characterized by allowing cross-linking ions to diffuse from a large outer reservoir into an alginate solution. The simplest way to obtain the diffusion-set gel is dripping the alginate solution into a copious solution of cross-linking cations, which yields alginate gel beads. The diffusion-set gel is also obtained by a dialysis of the alginate solution into cation solutions. The internal setting method is based on the use of an inactivated form of calcium (e.g., $CaCO_3$, Ca-EDTA) that is mixed with the alginate solution. The controlled release of the cross-linking cations is usually attained by means of a decrease of pH caused by the addition of slowly hydrolyzing molecules such as δ-gluconolactone.

The physical properties of the alginate gels prepared by the diffusion setting method and the internal setting method have extensively been studied. It has been shown that the alginate gels by the diffusion setting method exhibit an inhomogeneous distribution of polymers: the polymer concentration is lower in the center of the gel than near the surface.[3−5] The development of the concentration gradient in the gel formation was studied theoretically[6] and has been explained by the fact that the gelling zone extends from the surface toward the internal sol phase. Because the activity of alginate will be equal to zero at the gel front, alginate molecules diffuse from the sol phase toward the gel front, inducing an increase in the concentration of alginate in the gel phase. On the other hand, the gels with a homogeneous distribution of alginate were obtained by the internal setting method.[7] Regarding the optical properties, Thiele et al. reported more than 50 years ago that alginate gel beads exhibited birefringence.[8] They observed Cu-alginate gel beads prepared by the diffusion setting method under crossed nicols and found that the beads showed a birefringence pattern with crossed dark lines. Based on this observation, it was claimed that the pattern was attributed to the alignment of the alginate molecules perpendicular to the direction of Cu^{2+} flow. Recently, the optical anisotropy of Ca-alginate gel obtained by the dialysis method has been taken advantage of

Received: February 16, 2011
Revised: April 9, 2011
Published: April 19, 2011

in the study of the kinetics of the gel formation. Because the boundary between the birefringent gel and the isotropic sol could be distinguished clearly under the observation with crossed polarizers, the displacement of the gel front line was measured precisely.[9]

The anisotropic structure of the alginate gel has not been studied in detail. Because the birefringence value depends both on the polymer concentration and the degree of polymer orientation, the birefringence measurements are less efficient in studying quantitatively the anisotropic structure of the gels with the inhomogeneous distribution of polymers. In the present study, small-angle X-ray scattering (SAXS) experiments using synchrotron radiation were carried out to study the anisotropic structure of the Ca-alginate gels. In the SAXS measurements, both effects of the molecular orientation and the concentration of molecules can be directly determined because the degree of orientation is represented by the asymmetry of the two-dimensional SAXS patterns and the concentration effect is determined by the strength of SAXS intensity. There have been several studies by SAXS of Ca-alginate gels, but the anisotropic structure of the gel has not been studied so far.[10−13] Instead of spherical gel beads, cylindrical gels prepared within dialysis tubing in a high Ca^{2+}-concentration external bath were used in this study because the measurements with strips of gel samples with different slicing planes at different positions enable us to determine the axis of rotational symmetry of the anisotropic structure correctly and to estimate the degree of molecular orientation as a function of the radial position in the cylindrical gel. The objective of the present study is to characterize the anisotropic structure of the Ca-alginate gel prepared by the diffusion setting method by the combination of optical and SAXS measurements.

2. EXPERIMENTAL SECTION

2.1. Gel Preparation. Sodium alginate was purchased from Wako Pure Chemicals Industries, Ltd. and was used without further purification. The fraction F_G of α-L-guluronic acid and the fraction of diad sequences F_{GG}, F_{MG}, and F_{MM} were determined by high field ^{1}H NMR according to Grasdalen.[14] The values of F_G, F_{GG}, F_{MG}, and F_{MM} were 0.42, 0.27, 0.15, and 0.44, respectively. The viscosity of dilute solutions of the alginate sample in 0.1 M NaCl was measured at the temperature T = 20 °C and the intrinsic viscosity $[\eta]$ was determined to be 1.02×10^3 mL/g. The molecular weight M_w of the sample was estimated to be 2.5×10^5 using the Mark-Hauwink relation ($[\eta]$ (mL/g) = $4.85 \times 10^{-3} M_w^{0.97}$).[12] The distribution of molecular weights was not analyzed. The anisotropic gel of calcium alginate was prepared as follows: the alginate sample was dissolved in Milli-Q water and the alginate solutions of the concentrations C_{alg} = 2, 3, and 5 wt % were prepared. Each solution (60 g) was poured into a seamless cellulose tube with the diameter of 28 mm (Sanko Pure Chemical Co. Ltd.) and was dialyzed into 1 L of aqueous solution of 0.72 M calcium chloride (Wako Pure Chemicals Industries, Ltd.). After the dialysis at 25 °C for 6−9 h, a cylindrical gel was obtained. In the gel formation process, the flow direction of Ca^{2+} ions is along the radial direction of the cylindrical gel. To estimate the concentration profile of calcium alginate as a function of the distance x from the center, the gel was divided into four concentric layers with about 3 mm thickness with a precision less than 0.5 mm: each layer was cut circumferentially into pieces by a sharp knife and the pieces consisting of each layer were collected. The water content $\Delta W/W$ of each part of the gel was measured, where W is the weight of a portion of the gel and ΔW is the weight loss on the freeze-drying of the gel portion.

2.2. Optical Properties. A disk-shaped sample was prepared by slicing the cylindrical gel and used for the optical measurements. Optical anisotropy was detected by the observation under crossed nicols. The

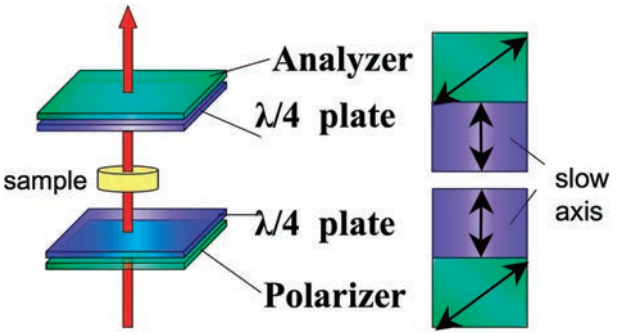

Figure 1. Arrangement of a pair of circular polarizers. A circular polarizer is depicted as two components of a polarizer (or an analyzer) and a quarter-wave plate. The sample is represented by a disk placed between the circular polarizers.

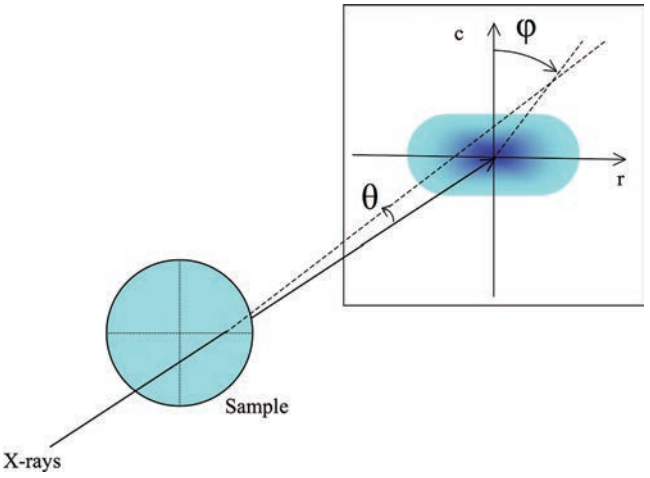

Figure 2. Schematic diagram of the experimental setup for the SAXS measurements and the definition of scattering angle θ and azimuthal angle φ. A disk-shaped sample is placed for the measurement of the incident X-ray beam direction of Z (see Figures 3 and 6a) as an example. An asymmetric SAXS pattern is illustrated schematically, and c and r axes are shown (see Figure 6a).

birefringence $|\Delta n|$ of the gel sample was measured as a function of the distance x from the center as follows. A He−Ne laser was used as a light source. The beam passed through a polarizer was incident on a desired position of the sample and the transmitted light was passed through an analyzer and then collected onto a photodiode. The value of retardation δ was determined from the measured intensities I and I_0 under crossed and open polarizers, respectively, by using a relation $I = I_0 \sin^2(\delta/2)$. Then the value of $|\Delta n|$ was calculated from a relation $|\Delta n| = (2\pi d/\lambda)\delta$, where d and λ are the thickness of the sample and the wavelength of the incident light, respectively.

To determine the birefringence sign of the gel and the direction of the molecular orientation, a pair of circular polarizers was arranged as shown in Figure 1. Suppose a birefringent sample with two refractive indices, n_1 and n_2, is placed between the circular polarizers with the principal axes corresponding to n_1 and n_2 directed parallel and perpendicular to the slow axis of the quarter-wave plates, respectively. When the sample was observed under natural light, it appears blue colored in the case of $n_1 > n_2$ and orange colored in the case of $n_1 < n_2$. The anisotropic gel sample and a fiber of sodium alginate used as a reference were observed under the circular polarizers. The fiber was spun from a solution of alginate of 2 wt % put into ethanol as a coagulation bath followed by drying in air.

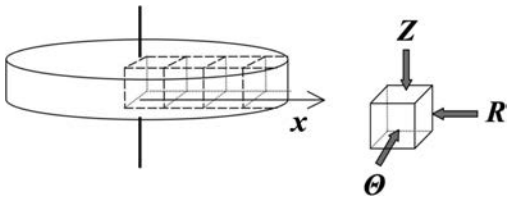

Figure 3. Directions of the X-ray beam incident on the sample in the SAXS measurements.

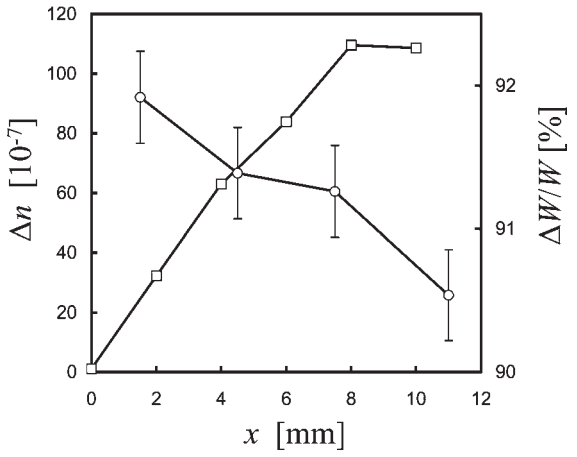

Figure 4. Water content $\Delta W/W$ (open circles) and birefringence $|\Delta n|$ (squares) of the Ca-alginate gel of C_{alg} = 2 wt % as a function of the radial distance x from the center of the gel.

2.3. Small-Angle X-ray Scattering. Small-angle X-ray scattering (SAXS) measurements were performed using the focusing small-angle diffractometer installed at the beamline 15A of the Photon Factory[15] at the High Energy Acceleration Research Organization in Tsukuba, Japan. Intense synchrotron radiation X-rays with wavelengths of 1.5 Å emitted from the positron storage ring were collimated and used for the SAXS measurements. The experimental setup for the SAXS measurements was schematically shown in Figure 2. The two-dimensional SAXS pattern was recorded with the area detector consisting of an image intensifier coupled to a CCD camera (model C7300, Hamamatsu Photonics). The spacial distortion and nonuniformity of the response of the detector were corrected following Itoh et al.[16] The background scattered intensity measured under the same experimental condition was subtracted from the scattered intensity of the sample. For the SAXS measurements, cross-section samples with 1 mm thick in different radial positions (x) from the center were prepared from the cylindrical gel.

To determine the axis of rotational symmetry of the anisotropic structure of the gel, the X-ray beam was incident on the gel sample at x = 7 mm from three different directions (Z, Θ, R) as shown in Figure 3. The direction of the incident beam is perpendicular to the direction of Ca^{2+} flow for the directions of Z and Θ and is along the flow for the direction of R. The dependence of SAXS intensity profiles on the distance x from the center of the gel was measured for the incident beam direction of Z. A sector-average was taken for the two-dimensional SAXS images in order to obtain the SAXS intensity profiles with a high S/N as functions of scattering angle θ and azimuthal angle φ defined in Figure 2.

3. RESULTS AND DISCUSSION

Figure 4 shows the water content $\Delta W/W$ and birefringence $|\Delta n|$ as a function of the distance x from the center of the Ca-alginate gel of C_{alg} = 2 wt %. The water content $\Delta W/W$ decreased slightly but certainly with x, indicating the concentration inhomogeneity of alginate molecules and calcium ions as the cross-linking agent along the radial direction of gel as reported in the previous studies.[3−5] The value of $\Delta W/W$ ranging from 90 to 92% was noticeably smaller than the initial value of the water content (98%) of the alginate solution. The difference would be due to the calcium ions as a nonevaporated component and a slight shrinkage of the alginate gel observed during the dialysis. Birefringence $|\Delta n|$ also depended on x: $|\Delta n|$ near the surface of the gel was higher than in the center of the gel and the value of $|\Delta n|$ at the center was almost zero. The lower value of $|\Delta n|$ near the center of the gel could be due to the lower concentration of the polymers or/and to the lower degree of polymer orientation.

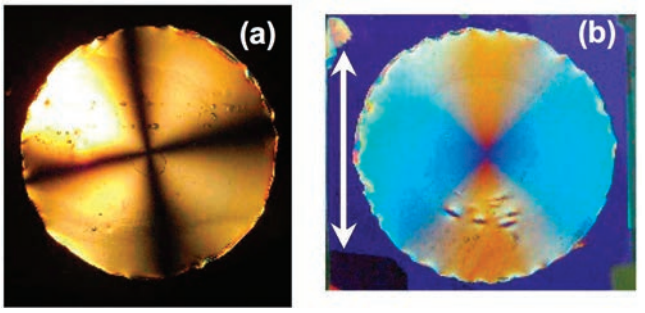

Figure 5. Photographs of the Ca-alginate gel of C_{alg} = 2 wt % observed under crossed nicols (a) and under a pair of circular polarizers (b). The arrow in (b) represents the direction of the slow axis of the quarter wave plates (see Figure 1). The diameter of the gel is 24 mm.

Photographs of the Ca-alginate gel of C_{alg} = 2 wt % observed under crossed nicols and under a pair of circular polarizers are shown in Figure 5a and b, respectively. In Figure 5a, a birefringence pattern with crossed dark lines is observed. The pattern suggested that the alginate molecules are oriented either radially or circumferentially in the cylindrical gel.[8,9] In Figure 5b, a pattern of blue and orange colored sectors is observed, indicating that the radial component of the refractive indices is smaller than the circumferential component. In the observation of a fiber of sodium alginate under a pair of circular polarizers, the fiber appeared blue when it was placed parallel to the slow axis of the quarter wave plates and appeared orange when placed perpendicular to the slow axis, showing that the birefringence sign of alginate is positive. These results reveal that the alginate molecules align along the circumferential direction in the cylindrical gel, which is perpendicular to the direction of Ca^{2+} flow (see Experimental Section), as was claimed for the Cu-alginate gel by Thiele et al.[8]

Figure 6a−c show the SAXS patterns for the Ca-alginate gel of C_{alg} = 2 wt % measured for the different incident X-ray beam directions, Z, Θ and R, respectively (see Figure 3). The X-ray beam was incident on the position x = 7 mm from the center of the gel. Similar asymmetric SAXS intensity patterns were obtained for the directions of Z and Θ, and a symmetric pattern was observed for the direction of R. These results show that the axis of rotational symmetry of the anisotropic structure of the gel is the direction of R, that is, the radial axis of the cylindrical gel. Thus, it is suggested that the orientation distribution of alginate molecules is rotationally symmetrical about the direction of Ca^{2+} flow.

Figure 7 shows the SAXS intensity profiles along the two principal axes for the asymmetric pattern as in Figure 6a, where the intensity plots denoted as r and c correspond to those along the axes parallel to the radial and to the circumferential directions in

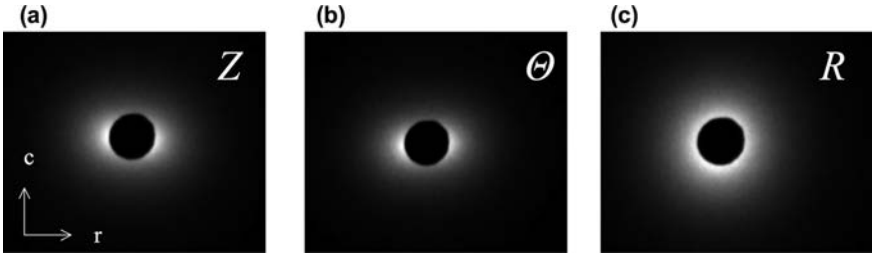

Figure 6. SAXS patterns for the Ca-alginate gel of C_{alg} = 2 wt % obtained for the incident X-ray beams from three different directions, Z, Θ and R, which are defined in Figure 2, are shown in (a), (b), and (c), respectively. In (a), the radial and circumferential directions in the cylindrical gel are shown as r and c, respectively.

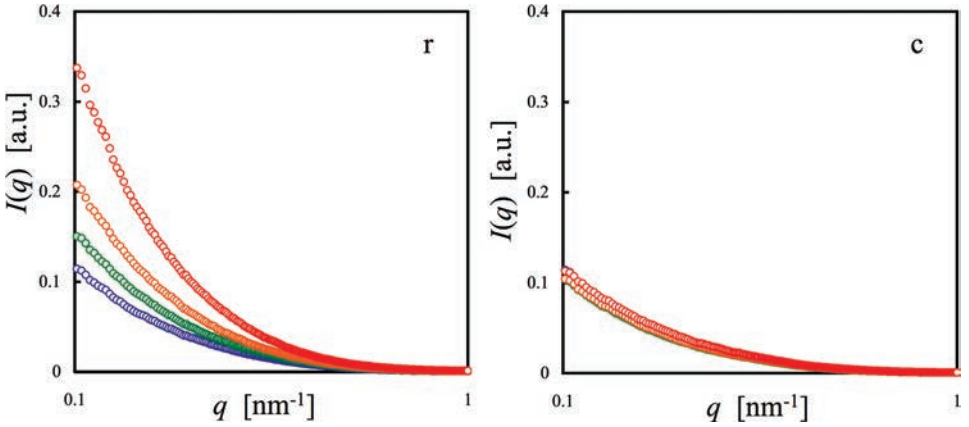

Figure 7. Intensity profiles of the SAXS pattern as in Figure 6a along the two principal axes. The directions of the axes are denoted as r and c, which are defined in Figures 2 and 6a. Scattered intensity ($I(q)$) is plotted against the scattering vector q. The intensity data was obtained at x = 0 (blue), 3 (green), 7 (yellow), and 10 mm (red) from the center of the gel, respectively.

the cylindrical gel, respectively. In other words, the directions of r and c are parallel and perpendicular to the direction of Ca^{2+} flow, respectively. The directions of r and c are also depicted in Figure 2. The plots in Figure 7 are shown in the form of the scattered X-ray intensity $I(q)$ versus the scattering vector q, defined as $q = 4(\pi/\lambda)\sin(\theta/2)$, where θ is the scattering angle. The different colors are used to distinguish the data obtained at the different positions of the gel. In the plots of the direction of r, $I(q)$ at low q was higher near the surface of the gel than in the center. On the other hand, $I(q)$ was almost independent of the distance from the center in the plots of the direction of c. At the center of the gel (x = 0 mm), the SAXS profiles for the directions of r and c coincided with each other. The results show that the asymmetry of the SAXS pattern is more significant near the surface than in the center and the gel is almost isotropic in the center. The SAXS intensity profiles indicated that the x dependence of $|\Delta n|$ in Figure 4 was not only due to the distribution of the polymer concentration but also to the x dependence of the degree of polymer orientation.

To characterize the microscopic structure of the gel, symmetric SAXS intensity profiles obtained at the center (x = 0 mm) of the gels were analyzed by the Kratky plots (i.e., $q^2I(q)$ vs q plots). Figure 8a shows the Kratky plots of the SAXS data for the gels of C_{alg} = 2, 3, and 5 wt %. The plots had a maximum at low q and then decreased with increasing q; the shape of the plots was reminiscent of that for the structure factor for a rigid rod-like particle (see below), implicating the formation of cylindrical rod structures in the central isotropic phase of the gel. The maximum was higher and shifted toward low q with the increase of C_{alg}. The maxima for C_{alg} = 2, 3, and 5 wt % occurred at q_m = 0.24, 0.22, and 0.20 nm^{-1}, respectively.

For a cylinder with the length L and the radius r, the structure factor (the normalized squared amplitude of the Fourier transform) after averaging over all orientations is described as

$$S_C(q) = \int_0^{\pi/2} \frac{\sin^2[q(L/2)\cos\gamma]}{[q(L/2)\cos\gamma]^2} \frac{J_1^2(qr\sin\gamma)}{(qr\sin\gamma)^2} \sin\gamma\, d\gamma \quad (1)$$

in which J_1 is the first-order Bessel function of the first kind with an argument of $qr\sin\gamma$, where γ is the cosine of the angle between $\boldsymbol{q}$ and the cylinder axis, and $S_C(0) = 1$.[17] For $1/L < q < 1/r$, eq 1 can be simplified and is described by

$$S_C(q) = \frac{\pi}{qL}\exp(-s^2q^2/2) \quad (2)$$

where s is the radius of gyration of the cross-section of the cylinder and $s = r/\sqrt{2}$. According to eq 2, s can be derived by $s = 1/q_m$. By application of this formula the radius r of the cylindrical rod particles for C_{alg} = 2, 3, and 5 wt % was estimated on average as 5.8, 6.4, and 7.1 nm, respectively. Because the values of the radius r are much larger than that of a single chain of alginate ($r \sim 0.3$ nm[11]), the rod-like particles observed in the SAXS measurements would be correspond to fibrils composed of a few tens of alginate chains. Robitzer et al. prepared the diffusion-set alginate gel by dripping the solution of alginate (F_G = 0.35) at C_{alg} = 1 wt % in the Ca^{2+} external bath at the concentration of 0.24 M and performed the SAXS measurements on the Ca-alginate gel beads. They indicated

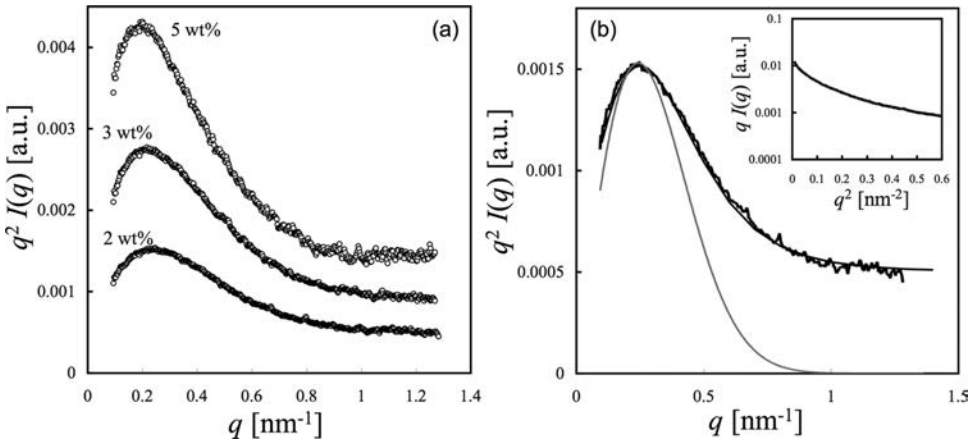

Figure 8. (a) Kratky plots for the SAXS intensities obtained at the center of the gel. The curves from the bottom to the top are for the Ca-alginate gels of C_{alg} = 2, 3, and 5 wt %, respectively. (b) The curves depicted by a gray line and a thin black line are given by eqs 2 and 4, respectively, and compared with the Kratky plot of the data for C_{alg} = 2 wt % in (a) (a thick black curve). In the inset, the experimental data are shown in the Guinier plot $qI(q)$ vs q^2 plot.

from the SAXS intensity profile that a structure of rod-like particles in the beads had a cross-sectional radius of ~5.1 nm, which is close to the present value obtained for C_{alg} = 2 wt %.[10] Stokke et al. studied the internal-set alginate gels by the SAXS measurements and showed that the cross-sectional radius of the rod-like structure increased with the stoichiometric ratio of $[Ca^{2+}]$, the concentration of Ca^{2+} in the gel to that of alginate. The cross-sectional radius for the internal-set gel of alginate (F_G = 0.39) of C_{alg} = 1 w/v% and $[Ca^{2+}]$ = 10 mM was ~1.5 nm.[12] The cross-sectional radius of the rod-like structure for the gels in the present study and in the study of Robitzer et al.[10] was larger than that in Stokke et al.[12] The difference would be attributed to rather high Ca^{2+}-concentrations of the external bath although the concentration of calcium ions in the gel was not determined in the present study. Thus, the gel formation of alginate by the addition of Ca^{2+} can be explained by the formation of rod-like fibrils due to interchain association induced by Ca^{2+}. In the generally accepted model which has been referred to as the egg-box model, the junction zones are formed in the gel by dimerization of polymer chains through Ca^{2+} coordination.[18] Recently, studies by X-ray fiber diffraction of Ca-alginate have been carried out[19,20] and a model for the formation of the junction zones was proposed. According to the model, polymer chains are packed on a hexagonal lattice with a lattice constant of ~0.66 nm, forming dimers of random pairs of chains through coordination of Ca^{2+} ions, and further lateral interaction between dimers is mediated by unspecific electrostatic interactions.[20] Thus, the rod-like particles observed in the present SAXS measurements could correspond to large fibrils formed by the unspecific lateral association of the junction zones involving the dimerization of the alginate chains.

In Figure 8b, the Kratky plot of SAXS data for C_{alg} = 2 wt % in Figure 8a is reproduced as a thick black curve. The inset of Figure 8b is the semilogarithmic plot of $qI(q)$ versus q^2 (i.e., a Guinier plot for the cross-section) for the data in Figure 8a. According to eq 2, the plot should yield a straight line around $q^2 \sim 1/s^2$. The obtained curved line suggests a distribution of the radii of gyration (s) of the cross sections of the rods. In Figure 8b, a Kratky plot of eq 2 with s = 4.1 nm (i.e., r = 5.8 nm; gray curve) is compared to the experimental data. The broader peak of the experimental curve again indicates the polydispersity of s. At high q, $q^2I(q)$ has a finite value almost independent of q suggesting $I(q) \sim q^{-2}$. This behavior could be interpreted as a contribution of a Gaussian coil component in the gel.[21] Therefore, the SAXS data indicate a coexistence of the rod-like fibrils and Gaussian coils in the gel. The structure factor for the Gaussian coil is written as[17]

$$S_G(q) = \frac{2}{q^4R_g^4}[\exp(-q^2R_g^2) - 1 + q^2R_g^2] \qquad (3)$$

Here, R_g is the radius of gyration of the Gaussian coil. For $qR_g \gg 1$, eq 3 is approximated as $S_G(q) \sim 2/(q^2R_g^2) \sim q^{-2}$. Thus, the SAXS intensity profile in the high q range ($q \gg 1/R_g$) in Figure 8b is approximated by the structure factor of Gaussian coil components.

For a coexistence of the fibrils and coils in the gel, the whole intensity profile can be represented by a superposition of the structure factors of a rod-like fibril and of a Gaussian coil. An empirical intensity equation can be set up from eq 2 with $g(s) = g_0e^{-\Gamma(s-\bar{s})^2}$ due to the effect of the distribution of s and eq 3 approximated for $q \gg 1/R_g$ as follows

$$I(q) = \frac{I_1}{q}\int_0^\infty \exp(-s^2q^2/2)g(s)\mathrm{d}s + \frac{I_2}{q^2} \qquad (4)$$

where I_1 and I_2 are constants related to the weight fraction of rods and coils, and $g(s)$ and $\bar{s}$ are a Gaussian distribution function of s and the mean value of s, respectively. This equation was applied to fit the observed intensity data. In eq 4, we assume an incoherent superposition of the structure factors of the rods and the coils.[21] The thin black curve in Figure 8b was described by eq 4 with appropriate values of the parameters used, which represents well the experimental data. The data for C_{alg} = 3 and 5 wt % in Figure 8a were also well represented by eq 4.

In consideration of the microscopic structure determined by the analysis of the SAXS intensity profiles obtained at the center of the gel, it is conjectured that the anisotropic structure of the Ca-alginate gel is attributed to the orientation of the fibrils composed of a few tens of alginate chains.

To quantify the degree of orientation of rod-like fibrils in the gel, the alignment factor A_f defined as

$$A_f = \frac{\int_0^{\pi/2} I(q,\varphi)\cos(2\varphi)\mathrm{d}\varphi}{\int_0^{\pi/2} I(q,\varphi)\mathrm{d}\varphi} \qquad (5)$$

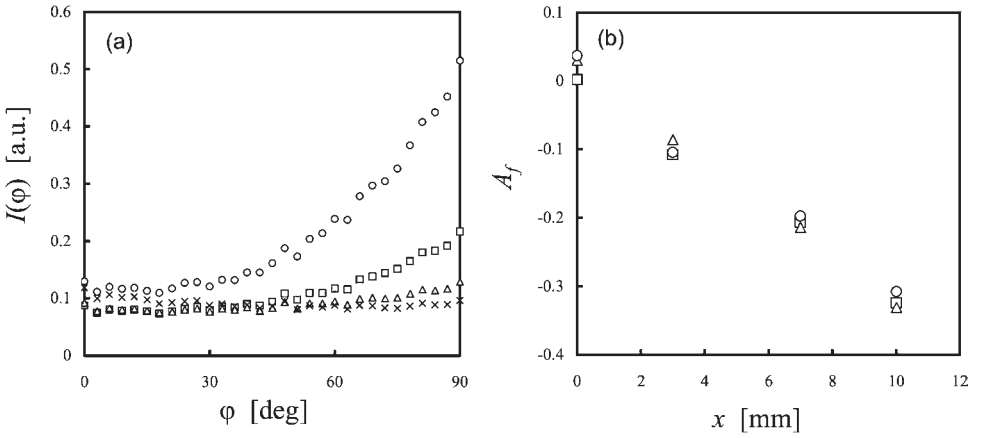

Figure 9. (a) SAXS intensities at $q = 0.1$ nm^{-1} are plotted against the azimuthal angle φ defined in Figure 2. The intensity data are obtained at $x = 0$ (crosses), 3 (triangles), 7 (squares), and 10 mm (circles) from the center of the gel of $C_{alg} = 2$ wt %, respectively. (b) Alignment factor A_f calculated by eq 5 as a function of the distance x from the center of the gel. The values are shown for the gels of $C_{alg} = 2$ (triangles), 3 (squares), and 5 wt % (circles), respectively.

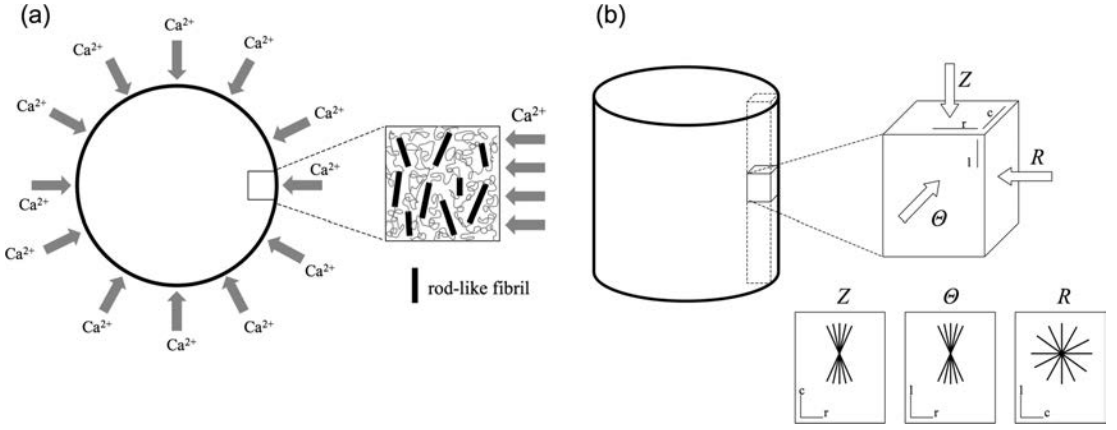

Figure 10. Illustration of the direction of Ca^{2+} flow and the fibril orientation in the cylindrical gel. (a) The top view of the cylindrical gel, depicting a relation of the direction of Ca^{2+} flow and the orientation of the rod-like fibrils formed in the gel. (b) The side view of the gel, depicting the orientational distribution of the fibrils in the part near the gel surface seen from three different directions (Z, Θ, and R). In the bottom, the isotropic orientation of the fibrils when viewed from the direction of R and the anisotropic orientation of the fibrils when viewed from the directions of Z and Θ are shown.

was calculated from the azimuthal variation of the SAXS intensity. The definition of the azimuthal angle φ is shown in Figure 2. The factor A_f has been used in the small-angle neutron scattering (SANS) and SAXS studies of anisotropic solutions of the rod-like molecules under shear flow.[22,23] Depending on the type of alignment, there are two different ranges of the factor. For an alignment of fibrils parallel to the radial direction of the cylindrical gel (parallel to the direction of Ca^{2+} flow), A_f ranges from 0 to 1 with $A_f = 1$ for the perfect alignment. For an alignment along the circumference (perpendicular to the direction of Ca^{2+} flow), A_f ranges from 0 to -1 with $A_f = -1$ for the fully oriented case. Full orientation, however, still allows an isotropic distribution of the rods about the axis of rotational symmetry. In the present case, the axis of rotational symmetry is the radial axis of the cylindrical gel, which is along the Ca^{2+} flow. In Figure 9a, the SAXS intensities at $q = 0.1$ nm^{-1}, which was arbitrarily chosen under the condition of $1/L < q < 1/r$, are plotted against φ for the Ca-alginate gel of $C_{alg} = 2$ wt % at different x. The result indicates that $I(\varphi)$ increases with increasing φ as leaving the center, confirming that the asymmetry in the SAXS pattern is more significant near the surface than in the center, as is shown in Figures 6 and 7. In Figure 9b, the values of A_f determined for the gels of $C_{alg} = 2$, 3, and 5 wt % are plotted against x. The results were almost independent of q values in the range $q < 1/r$. The value of A_f was almost zero at $x = 0$ and decreased almost linearly with x, indicating that the gel structure in the center is isotropic and the orientation of the rod-like fibrils is along the circumferential direction (perpendicular to the direction of Ca^{2+} flow). Figure 9b shows also that the x dependence of A_f is almost independent of C_{alg}. The value of A_f (~ -0.3) at $x = 10$ mm indicates still a large distribution of the overall fibril alignment near the surface of the gel.

It is difficult to elucidate the mechanism of the molecular orientation in the cylindrical gel from the present study. Woelki et al. studied the conformation of a polymer chain in the formation of a diffusion-set gel theoretically and suggested that the chain orientation is induced by the chain contraction in the direction of the gel growth.[24] The present SAXS results indicate that the anisotropic structure of the alginate gel is caused by the fibril formation of alginate chains in the direction perpendicular to the gel growth, not by the contraction of single polymer chains.

In the observation of the gel formation of alginate under the flow of Ca^{2+}, a sharp gelling front which separates a gel phase from a sol phase appears.[9] The sharp front line would be formed by strong interfacial tension between the gel phase and the sol phase. In other words, the chemical potential of alginate would change abruptly near the gel formation front. Because of the lower chemical potential at the gelling front, the alignment of more stretched alginate molecules along the gelling front would be preferably promoted, which may induce the fibril formation parallel to the front line. The decrease in the degree of fibril orientation near the center of the gel would be explained as follows. The shape of the front line is circular in the formation of the cylindrical gel and the radius of the gelling front is smaller near the center of the gel. Therefore the degree of orientation averaged in a finite observation area would be lesser near the center of the gel. Although the effect of the shape of the gelling front on the alignment factor A_f will be negligible near the surface of the gel, A_f becomes zero at the center of the gel, even if the fibrils are oriented perfectly along the front line.

Recently, it has been shown that optically anisotropic gels are formed by diffusion of gelation-inducing agents for various kinds of polymers such as polysaccharides (Curdlan,[25−28] κ-carrageenan,[29,30] carboxymethylcellulose,[31] and chitosan[32]), DNA,[33,34] and fibrous proteins.[35] It is necessary to study quantitatively the anisotropic structures of these gels with different types of cross-linking structure to elucidate the mechanism of the diffusion-induced anisotropic gel formation.

In summary, the present results are illustrated schematically in Figure 10. Figure 10a depicts the top view of the cylindrical gel, showing a relation of the direction of Ca^{2+} flow and the orientation of the rod-like fibrils formed in the gel. Figure 10b depicts the side view of the gel, showing the orientational distributions of the fibrils in the part near the gel surface seen from three different directions (Z, Θ, and R). The orientation of the fibrils is isotropic when viewed from the direction of R and those of the fibrils are anisotropic in the particular directions when viewed from the directions of Z and Θ.

4. CONCLUSION

The Ca-alginate gel with a cylindrical shape was prepared by the dialysis of the alginate solution into a high concentration Ca^{2+} solution, and the structure of the gel was studied by optical and SAXS measurements. The observation of the gel under crossed nicols and a pair of circular polarizers revealed that the molecular orientation was circumferential in the cylindrical gel. The asymmetric intensity pattern obtained for the alginate gel by SAXS measurements showed the anisotropic structure of gel and the SAXS patterns taken from different directions of incident X-ray beam indicated that the axis of rotational symmetry of the anisotropic gel structure was parallel to the radial direction (parallel to the direction of Ca^{2+} flow). The SAXS profiles at the different positions in the gel showed that the anisotropy was more significant near the surface than in the center of the gel. The analysis of the SAXS profile at the center of the gel indicated the formation of rod-like fibrils consisting of a few tens of alginate chains, suggesting that the anisotropic structure of the Ca-alginate gel is attributed to the orientation of the large fibrils mediated by unspecific interaction with Ca^{2+} ions. The alignment factor (A_f) estimated from the SAXS intensity data showed that the orientation of the fibrils was parallel to the circumferential direction (perpendicular to the direction of Ca^{2+} flow) in the gel and the degree of fibril orientation was more significant near the surface than in the center of the gel. The positional dependence of A_f was linear and almost independent of the concentration of alginate in the gel preparation.

AUTHOR INFORMATION

Corresponding Author

*Tel.: +81-277-30-1478. Fax: +81-277-30-1477. E-mail: maki@chem-bio.gunma-u.ac.jp.

ACKNOWLEDGMENT

The authors gratefully acknowledge Prof. K. Wakamatsu at Gunma University for the NMR measurements. This work was supported by KAKENHI (Grant-in-Aid for Scientific Research) on Priority Area "Soft Matter Physics" from the Ministry of Education, Culture, Sports, Science and Technology of Japan. The SAXS work has been approved by the Photon Factory Advisory Committee (Nos. 2007G002 and 2009G672).

REFERENCES

(1) Donati, I.; Paoletti, S. In *Alginate: Biology and Applications*; Rehm, B. H. A., Ed.; Springr-Verlarg Berlin; Heidelberg, 2009.

(2) Draget, K. I.; Smisrød, O.; Skjåk-Bræk, G. In *Polysaccharides and Polyamides in the Food Industry. Properties, Production, and Patents*; Steinbüchel, A., Rhee, S. K., Eds.; Wiley-VCH Verlag GmbH & Co. KGaA: Weinheim, 2005.

(3) Skjåk-Bræk, G.; Grasdalen, H.; Smisrød, O. *Carbohydr. Polym.* **1989**, *10*, 31–54.

(4) Thu, B.; Gåserød, O.; Paus, D.; Mikkelsen, A.; Skjåk-Bræk, G.; Toffanin, R.; Vittur, F.; Rizzo, R. *Biopolymers* **2000**, *53*, 60–71.

(5) Mørch, Ý. A.; Donati, I.; Strand, B. L.; Skjåk-Bræk, G. *Biomacromolecules* **2006**, *7*, 1471–1480.

(6) Mikkelsen, A.; Elgsaeter, A. *Biopolymers* **1995**, *36*, 17–41.

(7) Skjåk-Bræk, G.; Østgaard, K.; Smisrød, O. *Carbohydr. Polym.* **1991**, *14*, 159–178.

(8) Thiele, H. *Discuss. Faraday Soc.* **1954**, *18*, 294–314.

(9) Maki, Y.; Wakamatsu, M.; Ito, K.; Furusawa, K.; Yamamoto, T.; Dobashi, T. *J. Biorheol.* **2009**, *23*, 24–28.

(10) Robitzer, M.; David, L.; Rochas, C.; Di Renzo, F.; Quignard, F. *Langmuir* **2008**, *24*, 12547–12552.

(11) Wang, Z.-Y.; White, J. W.; Konno, M.; Saito, S.; Nozawa, T. *Biopolymers* **1994**, *35*, 227–238.

(12) Stokke, B. T.; Draget, K. I.; Smisrød, O.; Yuguchi, Y.; Urakawa, H.; Kajiwara, K. *Macromolecules* **2000**, *33*, 1853–1863.

(13) Yuguchi, Y.; Urakawa, H.; Kajiwara, K.; Draget, K. I.; Stokke, B. T. *J. Mol. Struct.* **2000**, *554*, 21–34.

(14) Grasdalen, H.; Larsen, B; Smisrød, O. *Carbohydr. Res.* **1979**, *68*, 23–31.

(15) Amemiya, Y.; Wakabayashi, K.; Itoh, K. *Photon Factory News* **1998**, *16*, 9-10. (In Japanese).

(16) Itoh, K.; Kamikubo, H.; Yagi, N.; Amemiya, Y. *Jpn. J. Appl. Phys.* **2005**, *44*, 8684–8691.

(17) Glatter, O.; Kratky, O. *Small Angle X-Ray Scattering*; Academic Press: New York, 1982.

(18) Grant, G. T.; Morris, E. R.; Rees, D. A.; Smith, P. J. C.; Thom, D. *FEBS Lett.* **1973**, *32*, 195–198.

(19) Li, L.; Fang, Y; Vreeker, R.; Appleqvist, I. *Biomacromolecules* **2007**, *8*, 464–468.

(20) Sikorski, P.; Mo, F.; Skjåk-Bræk, G.; Stokke, B. T. *Biomacromolecules* **2007**, *8*, 2098–2103.

(21) Gawronski, M.; Conrad, H.; Springer, T.; Stahmann, K.-P. *Macromolecules* **1996**, *29*, 7820–7825.

(22) Walker, L. M.; Wagner, N. J. *Macromolecules* **1996**, *29*, 2298–2301.

(23) Hongladarom, K.; Ugaz, V. M.; Cinader, D. K.; Burghardt, W. R.; Quintana, J. P.; Hsiao, B. S.; Dadmun, M. D.; Hamilton, W. A.; Butler, P. D. *Macromolecules* **1996**, *29*, 5346–5355.
(24) Woelki, S.; Kohler, H.-H. *Chem. Phys.* **2003**, *293*, 323–340.
(25) Dobashi, T.; Nobe, M.; Yoshihara, H.; Yamamoto, T.; Konno, A. *Langmuir* **2004**, *20*, 6530–6534.
(26) Nobe, M.; Kuroda, N.; Dobashi, T.; Yamamoto, T.; Konno, A.; Nakata, M. *Biomacromolecules* **2005**, *6*, 3373–3379.
(27) Nobe, M.; Dobashi, T.; Yamamoto, T. *Langmuir* **2005**, *21*, 8155–8160.
(28) Dobashi, T.; Yoshihara, H.; Nobe, M.; Koike, M.; Yamamoto, T. *Langmuir* **2005**, *21*, 2–4.
(29) Narita, T.; Tokita, M. *Langmuir* **2006**, *22*, 349–352.
(30) Narita, T.; Ohnishi, I.; Tokita, M.; Oishi, Y. *Colloids Surf., A* **2008**, *321*, 117–120.
(31) Lin, S. C.; Minamisawa, Y.; Furusawa, K.; Maki, Y.; Takeno, H.; Yamamoto, T.; Dobashi, T. *Colloid Polym. Sci.* **2010**, *299*, 695–701.
(32) Yamamoto, T.; Tomita, N.; Maki, Y.; Dobashi, T. *J. Phys. Chem. B* **2010**, *114*, 10002–10009.
(33) Dobashi, T.; Furusawa, K.; Kita, E.; Minamisawa, Y.; Yamamoto, T. *Langmuir* **2007**, *23*, 1303–1306.
(34) Furusawa, K.; Minamisawa, Y.; Dobashi, T; Yamamoto, T. *J. Phys. Chem. B* **2007**, *51*, 14423–14430.
(35) Furusawa, K.; Saito, H.; Tsugueda, A.; Narazaki, Y.; Yamamoto, T.; Dobashi, T. *Trans. Mater. Res. Soc. Jpn.* **2008**, *33*, 467–469.